The Journal of Neuroscience, May 1, 1998, *18*(9):3433–3442

Muscle Response to Changing Neuronal Input in the Lobster *(Panulirus Interruptus)* Stomatogastric System: Slow Muscle Properties Can Transform Rhythmic Input into Tonic Output

Lee G. Morris and Scott L. Hooper

Neurobiology Program, Department of Biological Sciences, Ohio University, Athens, Ohio 45701

Slow, non-twitch muscles are widespread in lower vertebrates and invertebrates and are often assumed to be primarily involved in posture or slow motor patterns. However, in several preparations, including some well known invertebrate "model" preparations, slow muscles are driven by rapid, rhythmic inputs. The response of slow muscles to such inputs is little understood. We are investigating this issue with a slow stomatogastric muscle (cpv1b) driven by a relatively rapid, rhythmic neural pattern. A simple model suggests that as cycle period decreases, slow muscle contractions show increasing intercontraction temporal summation and at steady state consist of phasic contractions overlying a tonic contracture. We identify five components of these contractions: total, average, tonic, and phasic amplitudes, and percent phasic (phasic amplitude divided by total amplitude).

cpv1b muscle contractions induced by spontaneous rhythmic neural input *in vitro* consist of phasic and tonic components. Nerve stimulation at varying cycle periods and constant duty cycle shows that a tonic component is always present, and at short periods the muscle transforms rhythmic input into almost completely tonic output. Varying spike frequency, spike number, and cycle period show that frequency codes total, average, and tonic amplitudes, number codes phasic amplitude, and period codes percent phasic.

These data suggest that tonic contraction may be a property of slow muscles driven by rapid, rhythmic input, and in these cases it is necessary to identify the various contraction components and their neural coding. Furthermore, the parameters that code these components are interdependent, and control of slow muscle contraction is thus likely complex.

Key words: Panulirus interruptus*; lobster; crustacea; stomatogastric; pylorus; pyloric network; slow muscle; tonic muscle; muscle contraction amplitude; contraction amplitude coding; temporal summation; motor control*

Muscle responses to neural input range from the rapid twitch contractions of vertebrate fast muscle to the graded, extremely slow contractions of some invertebrate muscle. Muscle type might be expected to match the dynamics of the motions that the muscle produces, and in some systems this is observed (Atwood, 1973; Rome et al., 1988). For instance, fast movements (e.g., startle response, fast swimming in fishes) often involve fast fiber activation, and slow movements (e.g., slow swimming in fish, maintenance of posture) involve slow fiber activation (Atwood, 1973; Webb, 1994). However, invertebrate and lower vertebrate muscles that can take seconds to fully contract and relax often receive comparatively fast (e.g., 1 sec cycle period) rhythmic neural inputs (Atwood, 1973; Hetherington and Lombard, 1983; Carrier, 1989; Morris and Hooper, 1997). In general, such slow muscles could not faithfully follow these patterns because they would not fully relax between inputs, and their contractions instead would temporally summate.

Previous research on slow muscles driven by rapid rhythmic inputs has (1) ignored temporal summation (Selverston and Moulins, 1987; Harris-Warrick et al., 1992; Hedwig, 1992), (2) acknowledged that summation exists without considering in detail the consequences for motor pattern control that it entails (Bullock, 1943; Josephson and Stokes, 1987; Tu and Dickinson, 1994), or (3) investigated ways to decrease summation to allow slow muscles to faithfully follow rapid patterns (Mason and Kristan, 1982; Hall and Lloyd, 1990; McPherson and Blankenship, 1992; Weiss et al., 1992). However, what appear to be temporally mismatched muscles are present in various systems, and it is possible that in many systems contraction temporal summation is behaviorally relevant. Temporally summated contractions would consist of phasic contractions with an underlying baseline contracture; how nervous systems could control these two interdependent components is unknown.

We have investigated these issues in a slow muscle of the lobster pylorus. Little is known about pyloric movements, but they had been assumed to be rhythmic because the pyloric neural network is rhythmic (Turrigiano and Heinzel, 1992). We show here, however, that when this muscle is rhythmically stimulated with constant duty cycle trains at behaviorally relevant cycle periods, its isotonic contractions show dramatic temporal summation. This summation is large enough that at rapid periods the muscle transforms rhythmic input into primarily tonic output. We show further that phasic amplitude depends primarily on the number of spikes within motor neuron bursts, the percent of the total amplitude that is phasic depends primarily on cycle period, and tonic, total, and average amplitudes depend primarily on burst spike frequency.

Some of these data have been published previously in abstract form (Morris and Hooper, 1994, 1996).

Received Jan. 5, 1998; revised Feb. 12, 1998; accepted Feb. 16, 1998.

This research was supported by grants to S.L.H. from the National Science Foundation, the Human Frontier Science Program, and Ohio University and its research council. We thank R. A. DiCaprio for discussion and advice, H. L. Atwood for the extremely kind donation of micromanipulators, and J. B. Thuma for extraordinary technical assistance.

Correspondence should be addressed to Scott L. Hooper, Neurobiology Program, Department of Biological Sciences, Irvine Hall, Ohio University, Athens, OH 45701.

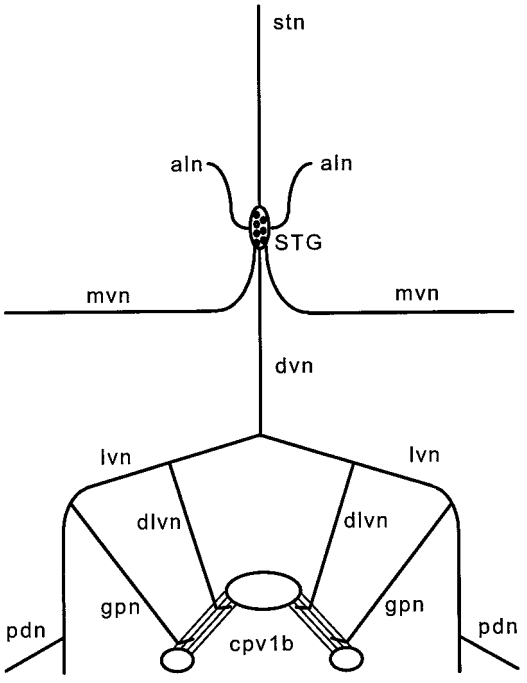

Figure 1. Schematic of a fully dissected cpv1b neuromuscular preparation. The cpv1b muscle originates on the hypodermis/carapace (*large oval, center*) and inserts on a pair of ossicles on the dorsal pyloric stomach (*small ovals*). Muscle contractions were measured by attaching a movement transducer to the hypodermis between the muscle pair with a wire hook. The muscles are innervated by the two Pyloric Dilator (PD) neurons, the cell bodies of which originate in the stomatogastric ganglion (*STG*) and project to the muscles via the dorsal ventricular (*dvn*), lateral ventricular (*lvn*), and dorsal lateral ventricular (*dlvn*) and/or gastropyloric (*gpn*) nerves. The pyloric dilator nerve (*pdn*) also carries branches of the PD axons; it and the *lvn* were used to stimulate and record nerve impulses. *aln*, Anterior lateral nerve; *mvn*, median ventricular nerve; *stn*, stomatogastric nerve.

METHODS AND MATERIALS

Spiny lobsters (500–1000 gm) were obtained from Don Tomlinson (San Diego, CA) and maintained in aquaria with chilled (12°C) circulating artificial sea water. Stomachs were dissected out of the animals in the standard manner (Selverston et al., 1976), except that the origin of the dorsal dilator (cpv1b) muscle pair was preserved on the hypodermis. Special care was taken to ensure that digestive juices never contacted the muscles and that the muscles were never stretched. Preparations were superfused continuously with chilled (12–15°C), oxygenated *Panulirus* saline with 40 mM glucose. The data shown here are from 12 experiments.

The dorsal dilator (cpv1b) muscles are a bilaterally symmetric muscle pair inserting on the medial dorsal surface of the pylorus and originating on the dorsal carapace (Fig. 1). They are innervated by the two Pyloric Dilator (PD) neurons (Maynard and Dando, 1974), which travel to the muscles through the dorsal ventricular (dvn), lateral ventricular (lvn), and dorsal lateral ventricular (dlvn) and/or gastropyloric (gpn) nerves. Contractions were produced by either ongoing pyloric network activity or stimulation of the lvn or the pyloric dilator (pdn) nerve (which also contains PD neuron axons) after the dvn was cut to prevent spontaneous pyloric network activity from reaching the muscle.

All electronics were standard. Extracellular nerve recordings and stimulations were made with polyethylene suction electrodes. Stimulation voltages were increased until maximum muscle contraction amplitudes were achieved, and hence presumably both motor neuron axons were being stimulated. Intracellular neuronal recordings were made with glass microelectrodes filled with 0.55M K_2SO_4, 0.02M KCl (resistance 10–20 MΩ), and an Axoclamp 2A. Contractions were measured by attaching a Harvard Apparatus 60-3000 isotonic transducer to a wire hooked through the hypodermis between the cpv1b muscle pair. Rest muscle length was maintained at approximately physiological levels.

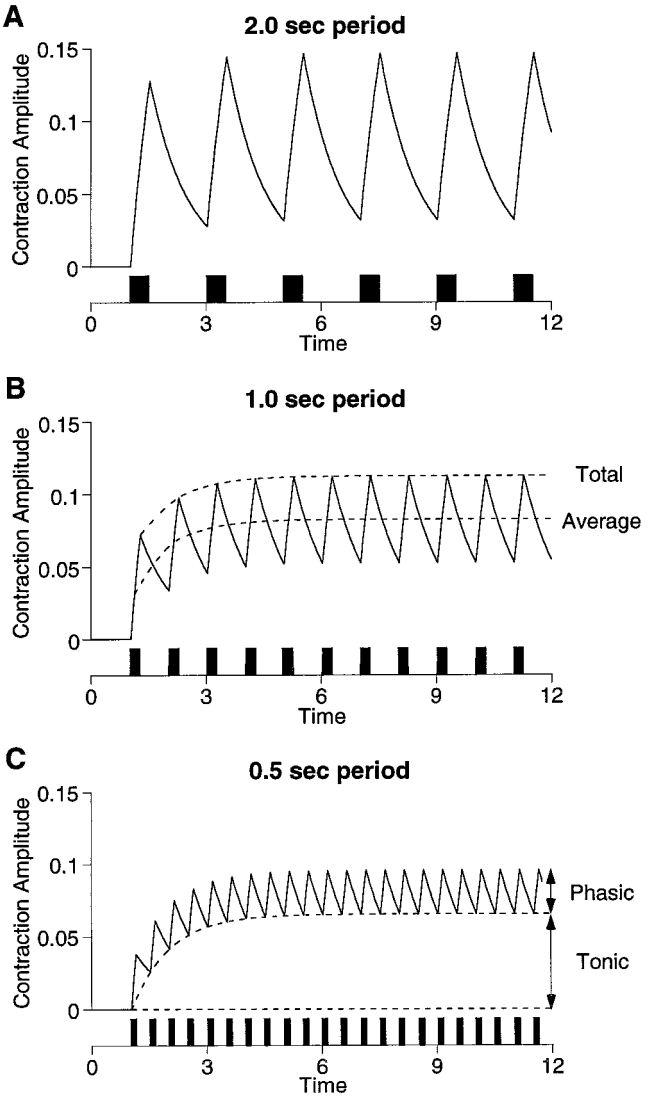

Figure 2. Simple model of a slow, non-twitch muscle undergoing rhythmic contractions at various cycle periods with constant intraburst spike frequency (30 Hz) and duty cycle (0.25). *A*, Slow (2 sec period) rhythmic neural input (*boxes* represent bursts of spikes) allows the muscle sufficient time to relax almost fully between neural bursts; the muscle thus can faithfully follow the neural pattern. *B, C*, As cycle period decreases (*B*, 1 sec; *C*, 0.5 sec), the contractions show increasing summation. Five quantitative measures can be identified: *Total* and *Average* (the amplitude around which the muscle oscillates, calculated at 50% of phasic amplitude) amplitudes (*B*), *Phasic* and *Tonic* amplitudes (*C*), and percent phasic (phasic amplitude divided by total amplitude; not shown). Spike numbers: *A*, 16; *B*, 8; *C*, 4; contraction amplitude induced by a single spike: 0.01; relaxation rate (τ): 1 sec.

Muscle loading was determined by observing single contractions elicited by nerve stimulation with physiologically relevant bursts of action potentials. We consistently found that loads that produced the largest muscle contractions were often insufficient to return the muscle to its rest length. Muscle load was therefore adjusted to achieve the maximum contraction amplitude at which the muscle fully relaxed to rest length after the stimulation. A support bar was then placed under the end of the transducer arm to prevent muscle overstretching between contraction trains. Transducer output was amplified 20- to 50-fold by a Tektronix AM502 differential amplifier. Contraction parameters were measured using Spike II (Cambridge Electronics Design) and Kaleidagraph (Synergy Software) after transfer (Cambridge Electronics Design 1401 laboratory interface) to a Gateway 2000 P5. Figure 2 was made using a model developed with Stella II (High Performance Systems) software. Statistics

were performed with either JMP (SAS Institute Inc.) or SPSS, Inc., software.

RESULTS

To appreciate the difficulties that arise when slow muscles are driven by comparatively rapid neural inputs, consider the simple model of a slow, non-twitch muscle shown in Fig. 2. Each motor neuron spike induces a constant amplitude unitary muscle contraction, muscle relaxation is a single exponential, and duty cycle (the percentage of the cycle occupied by the neuronal burst) and intraburst spike frequency are constant.

When the rhythm is slow (Fig. 2*A*), the muscle has time to relax almost fully between individual neuron bursts, and muscle movement therefore faithfully follows the neural pattern. As cycle period decreases (Fig. 2*B,C*), the muscle has less time to relax before the next neuron burst. As a consequence, the initial muscle contractions in the train temporally summate, and total contraction amplitude increases. Because the relaxation is exponential [$Amp(t) = Amp_{tot} \cdot e^{-t/\tau}$, where t is reset to 0 at the peak of each contraction (Amp_{tot})], the slope of the relaxation ($dAmp/dt = -(Amp_{tot}/\tau) \cdot e^{-t/\tau}$) depends on Amp_{tot}. Thus, as the contractions increasingly summate, and hence total contraction amplitude increases, the relaxation slope steepens (compare the relaxation after the first contraction with those after the later contractions in Fig. 2*C*). As a result, the magnitude of the relaxation that occurs during each interburst interval becomes greater, and this process continues until interburst relaxation magnitude equals contraction amplitude.

In this steady-state condition, muscle contraction consists of (Fig. 2*C*) a *phasic* component (the rhythmic muscle contraction that follows the neural input) and a *tonic* component (the minimum contraction to which the muscle relaxes between neuron bursts). In the model, both phasic and tonic component contraction amplitudes change as the cycle period changes. In slow period trains, phasic amplitude is large because of the large number of spikes in each neuron burst, and tonic amplitude is small because of the long interburst interval. As cycle period decreases, phasic amplitude decreases (due to the decrease in spike number/burst), and tonic amplitude increases (due to the decrease in interburst interval). The relative contributions of the phasic and tonic components to the total contraction of the muscle were quantified by expressing the phasic component as a percentage of total contraction amplitude (percent phasic; percent tonic would equal 1 − percent phasic).

Two other parameters of the contraction train at steady state are average (the mean amplitude about which the phasic contractions of the muscle oscillate) and total amplitude (Fig. 2*B*). In the model, the total amplitude changes as period changes, whereas the average amplitude does not. The average remains constant because the phasic and tonic amplitudes vary inversely; as cycle period decreases, phasic amplitude decreases, tonic amplitude increases, and hence average amplitude remains stable.

This model is simplistic, but it does show that temporal summation in response to rhythmic neural input is possible in slow muscles. It also suggests that full characterization of slow muscle contractions requires measuring at least percent phasic and average, total, tonic, and phasic amplitudes.

We have investigated slow muscle responses using the dorsal dilator (cpv1b) muscle of the crustacean pyloric neuromuscular system. The dorsal dilator muscle is innervated by the two electrically coupled PD motor neurons of the rhythmically active pyloric neural network (Maynard and Dando, 1974). In a manner similar to that shown in Fig. 2, this network approximately maintains phase as the cycle period is varied (Hooper, 1997). Figure 3*A* shows PD neuron activity at three cycle periods (*top* to *bottom*, 0.4, 0.6, and 1.1 sec); note that PD neuron burst duration increases (*top* to *bottom*, 0.12, 0.18, and 0.33 sec) sufficiently to approximately maintain duty cycle (0.3, all traces).

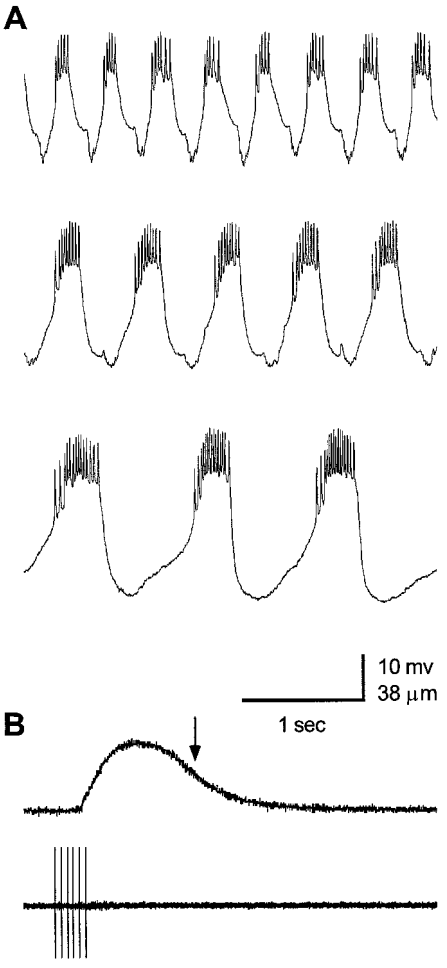

Figure 3. cpv1b muscle response is slow compared with pyloric cycle periods. *A*, Intracellular PD neuron recordings at three periods (*top* to *bottom*, 0.40, 0.60, 1.1 sec). As period increases, burst duration (0.12, 0.18, 0.33 sec, respectively) increases sufficiently to maintain PD neuron duty cycle (0.3). Note that increased burst duration results in increased spike number per burst. *B*, cpv1b muscle contraction in response to a 0.25 sec, 30 Hz stimulus train, on the same time scale as the recordings in *A*. Muscle contraction and relaxation are slow; if the muscle was driven at a 1 sec period, which is typical for this burst duration, the muscle will not fully relax before the next contraction begins (*arrow*).

Stomatogastric muscles are slow, non-twitch muscles that can take seconds to fully contract and relax (Hoyle 1953, 1983; Atwood and Hoyle, 1965; Govind et al., 1975; Atwood et al., 1977, 1978; Morris and Hooper, 1997). Figure 3*B* shows an isotonic contraction of a dorsal dilator muscle in response to a 0.25 sec, 30 Hz stimulus train applied to the lvn. Disregarding the delay to contraction, full muscle contraction and relaxation to this stimulus take ~2 sec. If the muscle were being driven by a 1 sec cycle period rhythmic train, the next contraction (assuming that delay to contraction did not change) would start 1 sec after the beginning of the first contraction (*arrow*), and hence would occur before the muscle relaxed completely. Periods of 1 sec are well

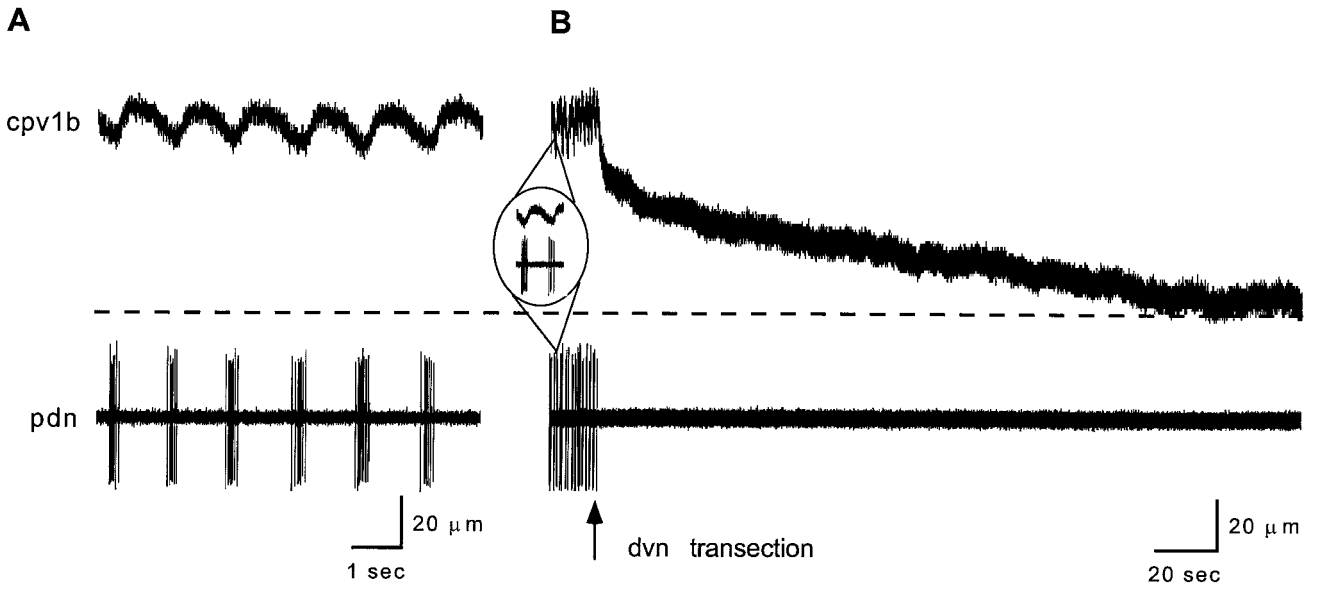

Figure 4. cpv1b muscle shows temporal summation of contractions in response to centrally generated rhythmic neural input. *A*, cpv1b muscle rhythmic contractions (*top*) in response to PD neuron bursts (*pdn trace, bottom*). *B*, A later portion of the cpv1b muscle contraction and neural input shown in *A* on a compressed time scale (*inset*). When the *dvn* is transected (*arrow*), neural input to the muscle is eliminated (bursting stops, *bottom*), and the rhythmic contractions cease (*top*). The muscle slowly relaxes to a new baseline (*dashed line*) that is much lower than the lowest amplitude observed during the train (compare with *A*).

within the physiological range of the pyloric network; these considerations suggest that dorsal dilator muscle contractions may temporally summate in response to pyloric network input.

That this is so is shown in Figure 4. Figure 4*A* shows simultaneous recordings of dorsal dilator muscle contractions (*top trace*) and PD neuron activity (*pdn trace*) in a preparation in which the muscle was left attached to the neural network; muscle activity consists of small rhythmic PD neuron-timed contractions. When the muscle was disconnected from the network by dvn transection (Fig. 4*B, arrow*), PD neuron input was eliminated and rhythmic muscle contraction ceased. However, rather than simply relaxing to the seeming rest length in Fig. 4*A*, the muscle continued to lengthen slowly for >3 min (note time base change) and stabilized at a much lower amplitude (*dashed line*). This observation suggests that the muscle response shown in Fig. 4*A* consisted of relatively small rhythmic contractions overlying a large (in this case, almost three times greater than the rhythmic component) tonic contracture. Thus, at least *in vitro*, dorsal dilator muscle contractions temporally summate in response to spontaneous pyloric neural network activity.

To characterize the dependence of the various components of dorsal dilator muscle contractions on neural input parameters, we turned to nerve stimulation experiments (in which the dvn was transected) to be able to deliver stimulus input trains with various cycle periods, intraburst spike frequencies, and intraburst spike numbers. However, all work reported here was performed using constant duty cycle trains (0.25), because in the absence of neuromodulatory influences, the pyloric network is approximately duty cycle constant (Fig. 3) (Hooper, 1997).

Figure 5*A* shows isotonic contractions of the dorsal dilator muscle induced using physiologically relevant spike trains (2, 1, and 0.5 sec cycle periods, 60 Hz intraburst spike frequency). At the longest period, the muscle was primarily phasic, although a small tonic component was present (Fig. 5*A1*). As the period decreased, muscle response became increasingly tonic (Fig. 5*A2,A3*). The shortest period (0.5 sec) showed dramatic temporal summation (Fig. 5*A3*), and the total contraction amplitude of the muscle consisted largely of the tonic component.

Note that the dorsal dilator muscle shown in Fig. 5*A* did not completely reach steady state, even within 50 sec of rhythmic stimulation. In general, the response of this muscle consisted of an initial rapid (2–5 contractions) temporal summation followed by a very slow rise (attributable to facilitation of the phasic contraction component) that could continue for as long as 2–5 min before steady state was achieved completely (Morris and Hooper, 1996). In experiments in which such long trains were used, the muscles showed fatigue before sufficient trains could be delivered to fully characterize muscle response properties. We therefore instead used trains of at least 50 sec duration, because full temporal summation was well achieved within these times. To test for any confounding effects of the slow facilitation, we performed our data analyses at several times into the trains. Provided the analyses were performed after the full temporal summation had been achieved, in no case did the results of these analyses differ with respect to the time into the train (see below). Except where noted, in all cases shown here the data were taken at least 50 sec into the train.

Figure 5*B* shows averaged percent phasic data from 12 preparations. As expected from the data in Fig. 5*A*, dorsal dilator muscle contractions were not completely phasic at any cycle period. At the shortest period, the muscle was almost completely tonic (13 ± 14 percent phasic). As the period increased, percent phasic increased to 38 ± 21 at a 1 sec period, and to 66 ± 15 at a 2 sec period (all groups different at $p < 0.0001$; Kruskal–Wallis test).

These observations naturally led to the question of what neural input parameters code the various contraction amplitudes and percent phasic. We have shown previously that unlike higher vertebrate muscles in which amplitude is coded by intraburst spike frequency, the amplitude of individual dorsal dilator muscle

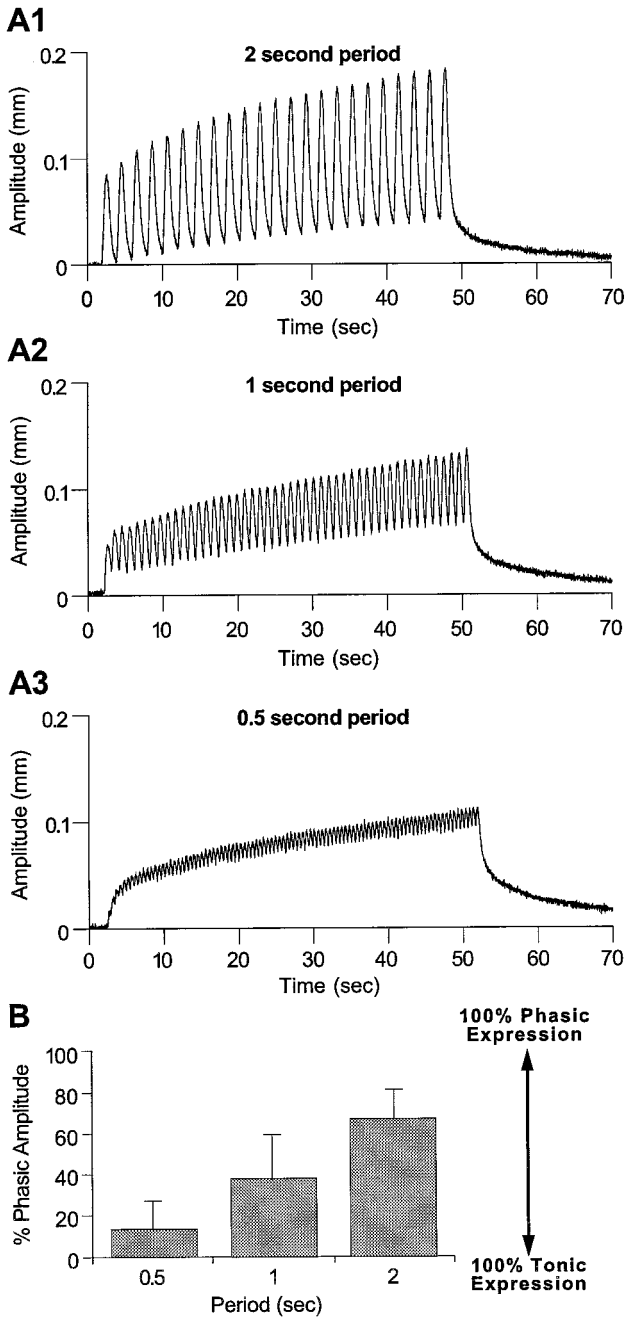

Figure 5. Changing cycle period alters the relative amounts of phasic and tonic components in cpv1b contractions. *A1–3*, As period decreases, contractions become less phasic and more tonic. *A1*, When stimulated at a 2 sec period, the muscle is primarily phasic, with only a small tonic component. *A2*, Decreasing period to 1 sec decreases the phasic component and increases the tonic component. *A3*, Decreasing period to 0.5 sec reduces the phasic component sufficiently that the muscle response is primarily tonic. *B*, Relative change in phasic and tonic components (the percent of the total amplitude which is phasic, *% Phasic*), as period changes ($n = 12$). Short periods have low percent phasic values, whereas longer periods have high percent phasic values. All groups are statistically different ($p < 0.0001$; Kruskal–Wallis test).

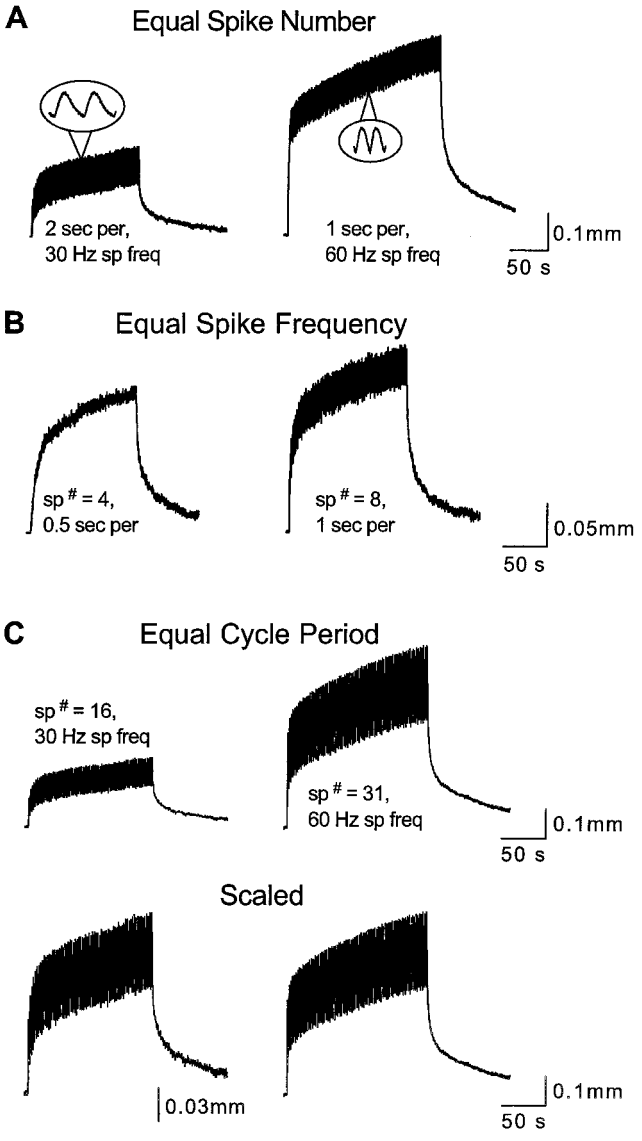

Figure 6. Different neural input parameters appear to code different contraction components. All trains are from the same experiment. *A*, Trains with the same intraburst spike number (16), but different intraburst spike frequencies (*left*, 30 Hz; *right*, 60 Hz) and cycle periods (2 and 1 sec; duty cycle 0.25), have the same phasic contraction amplitude (*insets*). *B*, Trains with the same intraburst spike frequency (30 Hz), but different intraburst spike numbers (4 and 8) and periods (0.5 and 1 sec; duty cycle 0.25), have approximately similar tonic, total, and average contraction amplitudes. *C*, Trains with the same period (2 sec; duty cycle 0.25), but different intraburst spike frequencies (30 and 60 Hz) and spike numbers (16 and 31), give the same percent phasic (*top*). This relationship is clearer when contraction total amplitudes are scaled (*bottom*).

contractions in response to physiological neural inputs is coded by burst spike number (Morris and Hooper, 1997). Because these previous methods for quantitatively distinguishing spike number versus spike frequency amplitude coding involved analyses of tetanic contractions, they are inappropriate for the rhythmic train data reported here. An alternative method is to (1) induce muscle contractions with trains containing various spike numbers, intraburst spike frequencies, and cycle periods, (2) plot all contraction components against spike number, spike frequency, and cycle period, and (3) determine which parameter best predicts each component.

Visual examination of contraction trains in which burst spike number, intraburst spike frequency, or cycle period were kept constant (Fig. 6; all trains are from the same experiment) sug-

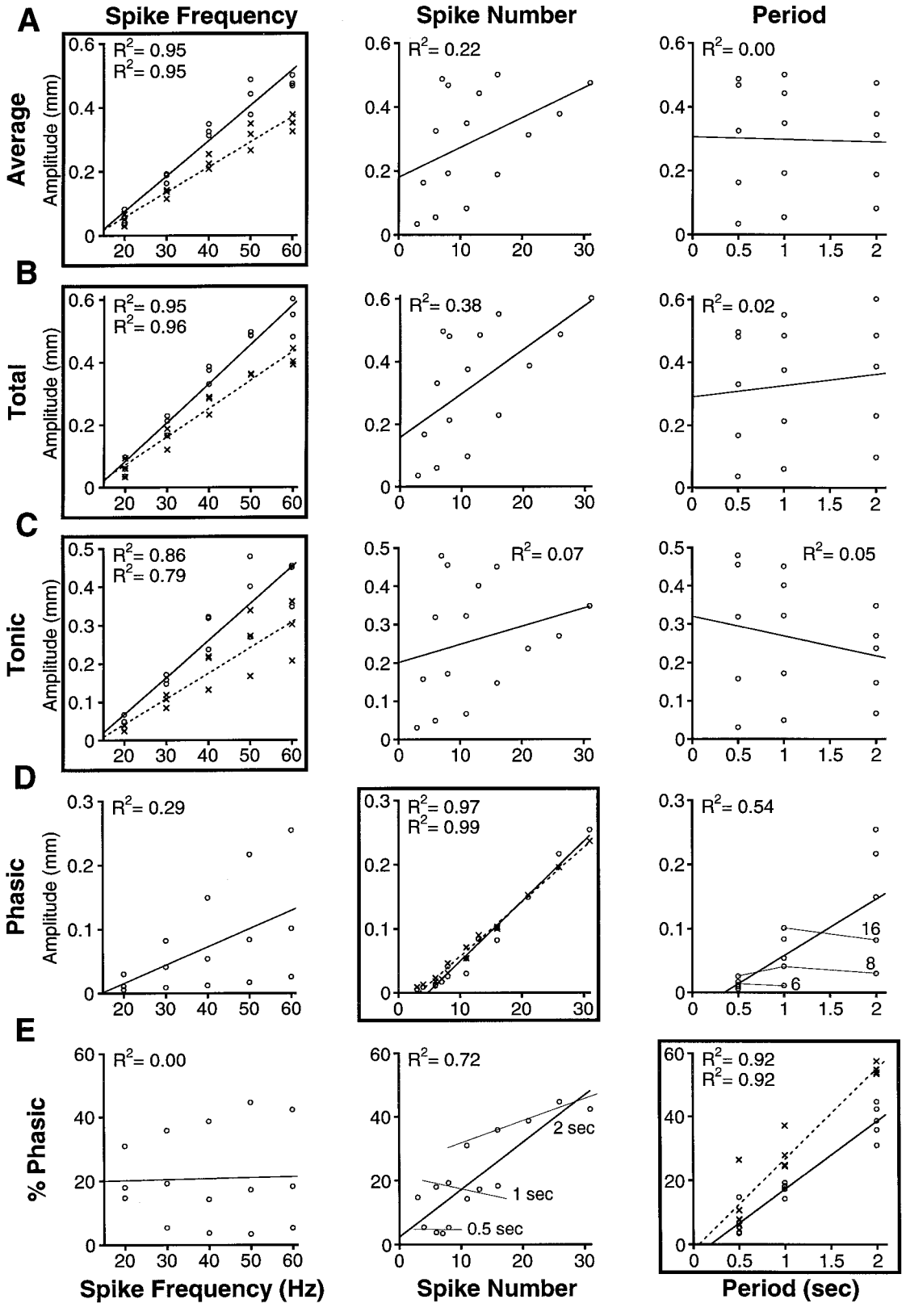

Figure 7. Intraburst spike frequency, intraburst spike number, and cycle period code for different aspects of cpv1b contractions in a single experiment. *A–C*, Intraburst spike frequency (*left column*) best codes for average (*A*), total (*B*), and tonic (*C*) amplitudes (*boxes*). *D*, Intraburst spike number (*middle column*) best codes for phasic amplitude (*box*). Period seems to code reasonably well for phasic amplitude (*right column*) ($R^2 = 0.54$), but there is large scatter around the best fit line, and points representing the same spike number (*numbers* on plot) have similar amplitudes despite their different periods (*fine lines*). Spike number is a function of cycle period, and this interdependence can produce misleading apparent correlations (see Results). *E*, Cycle period (*right column*) best codes for percent phasic (*box*). Again, the interdependence of spike number and period makes it (*Figure legend continues*)

gested that phasic amplitude is spike number dependent, tonic, average, and total amplitudes are spike-frequency dependent, and percent phasic is cycle-period dependent. Figure 6*A* shows two trains with the same burst spike number (16), one at a 2 sec period (*left*; burst duration 0.5 sec, intraburst spike frequency 30 Hz) and one at a 1 sec period (*right*; burst duration 0.25 sec, intraburst spike frequency 60 Hz). Phasic amplitude (*insets*) is similar in each train, but tonic, total, and average amplitudes, and percent phasic, are not. Figure 6*B* shows two trains stimulated with the same intraburst spike frequency (30 Hz), one at a 0.5 sec period (*left*; burst duration 0.125 sec, spike number 4), and one at a 1 sec period (*right*; burst duration 0.25 sec, spike number 8). The phasic amplitude and percent phasic of these trains are different, whereas their tonic, total, and average amplitudes are approximately similar.

The traces in Figure 6*C* show trains with the same cycle period (2 sec, burst duration 0.5 sec) but different intraburst spike frequencies (*left*, 30 Hz; *right*, 60 Hz) and hence different spike numbers (16 and 31, respectively). The two trains in the top and bottom rows are identical, except the upper trains are at the same scale, whereas the total amplitudes of the lower trains have been scaled to facilitate comparison of the percent phasic values. As can be easily observed in the lower traces, percent phasic is similar in both traces.

To verify these visual observations, linear fits to data from individual experiments were performed. Figure 7 shows the linear fits of the average (*A*), total (*B*), tonic (*C*), and phasic (*D*) amplitudes, and percent phasic (*E*), versus intraburst spike frequency (*left column*), spike number (*middle column*), and cycle period (*right column*) from one experiment. The plots surrounded by boxes show the best fits for each parameter examined. These plots also show the data points (*x*), fits (*dashed lines*), and R^2 values (lower values) from contractions only 20 sec into the train; it is apparent that although the slopes of the lines in some cases differ, the coding variable remains the same. As can be seen in Fig. 7*A–C*, spike frequency is the best predictor (highest R^2 value) of average, total, and tonic amplitudes, with R^2 values ranging from 0.79 to 0.96 (*left column, boxes*). These data suggest that all three of these parameters are primarily coded by spike frequency. Phasic amplitude and percent phasic (Fig. 7*D,E*), on the other hand, are not well predicted by spike frequency [*left column;* R^2 values, respectively, of 0.29 and 0.00 for the plotted (later in the train) data points; the 20 sec data plots are similar (data not shown)]. As suggested earlier, phasic amplitude is better predicted by spike number ($R^2 = 0.97$ and 0.99; *center column, box*) and percent phasic by cycle period ($R^2 = 0.92$ for both data sets; *right column, box*).

Although it is clear that spike number predicts phasic amplitude and cycle period predicts percent phasic, the apparent correlations of phasic amplitude with cycle period ($R^2 = 0.54$), and percent phasic with spike number ($R^2 = 0.72$), might indicate that these latter factors are also predictors. However, these apparent correlations may be misleading. Burst spike number ($sp^{\#}$) is a function of both intraburst spike frequency (*spfreq*) and burst duration ($sp^{\#} = int(spfreq \cdot burst\ duration) + 1$). However, burst duration equals duty cycle times cycle period, and thus spike number is intercorrelated with both spike frequency and period ($sp^{\#} = int(spfreq \cdot duty\ cycle \cdot period) + 1$).

A consequence of this intercorrelation is that (at a given spike frequency) as cycle period increases so does spike number and hence phasic amplitude (Fig. 7*D, right column*). Thus, to ascertain whether period independently affects phasic amplitude, it is necessary to compare data with different periods but identical spike numbers (*fine lines*; associated values are spike number). It is apparent that when the intercorrelation of spike number and period is removed, period does not significantly predict phasic amplitude (the *fine lines* are not parallel to the fit). Multiple step-wise regression (probabilities: *f*-to-enter ≤ 0.05, *f*-to-remove ≥ 0.10) performed on these data entered spike number as the first predictor ($R^2 = 0.97$; $p < 0.001$); the model also entered period and spike frequency, but the overall change in R^2 value (0.02) was negligibly small, and thus spike number is the primary coding factor for phasic amplitude.

The intercorrelation between spike number and cycle period similarly complicates interpretation of the percent phasic data (Fig. 7*E, middle column*). Thus, to ascertain whether spike number independently affects percent phasic, it is necessary to compare data with different spike numbers but identical periods (*fine lines*; associated values are periods). It is apparent that when the intercorrelation of spike number and period is removed, spike number does not significantly predict percent phasic (the *fine lines* are not parallel to the fit). Multiple step-wise regression performed on these data entered period as the only predictor ($R^2 = 0.92$; $p < 0.001$); period thus codes percent phasic.

Figure 8 shows mean R^2 values (five experiments) of the various linear fits shown in Fig. 7. It is apparent that spike frequency (*gray*) better predicts average, total, and tonic amplitudes ($R^2 = 0.87 \pm 0.12$, 0.81 ± 0.15, and 0.76 ± 0.14, respectively) than does spike number (*hatched;* $R^2 = 0.15 \pm 0.05$, 0.35 ± 0.06, and 0.03 ± 0.03, respectively) or cycle period (*black;* $R^2 = 0.01 \pm 0.01$, 0.05 ± 0.04, and 0.15 ± 0.11, respectively). These data thus suggest again that average, total, and tonic contraction amplitudes are primarily coded by spike frequency.

As was also seen in the data from an individual experiment (Fig. 7), spike number best predicts phasic amplitude (*hatched;* $R^2 = 0.88 \pm 0.10$), but a relatively large apparent contribution of period is also present (*black;* $R^2 = 0.52 \pm 0.11$). However, when multiple step-wise regressions were performed on normalized (to compensate for individual variation; each experiment was normalized to 1 sec period, 60 Hz values) grouped data, spike number was entered as the first predictor ($R^2 = 0.81$; $p < 0.001$). The model also later entered spike frequency and period, but the overall change in R^2 value (0.04) was negligibly small, and thus spike number is the primary coding factor for phasic amplitude. Similarly, cycle period best predicts percent phasic (*black;* $R^2 = 0.89 \pm 0.07$), but a large apparent contribution of spike number is also present (*hatched;* $R^2 = 0.66 \pm 0.14$). However, multiple step-wise regressions performed on normalized, grouped data entered only period into the model ($R^2 = 0.70$; $p < 0.001$). Dependence of percent phasic on period is most likely attribut-

←

appear that spike number also codes reasonably well for percent phasic ($R^2 = 0.72$). However, there is large scatter around the best fit line, and points representing the same period (*numbers* on plot) have similar amplitudes despite their different spike numbers (*fine lines*; see Results). *Open circles, solid lines*, and *upper* R^2 values are data from late in the trains; *x* points, *dashed lines*, and *lower* R^2 values (only in *boxed plots*) are data from 20 sec in the train; note that in all cases the data from both sets well predict the variable in question. When 20 sec data are plotted versus the other, poorly predicting parameters, the same pattern of scatter and similar R^2 values are observed as with the later data (data not shown).

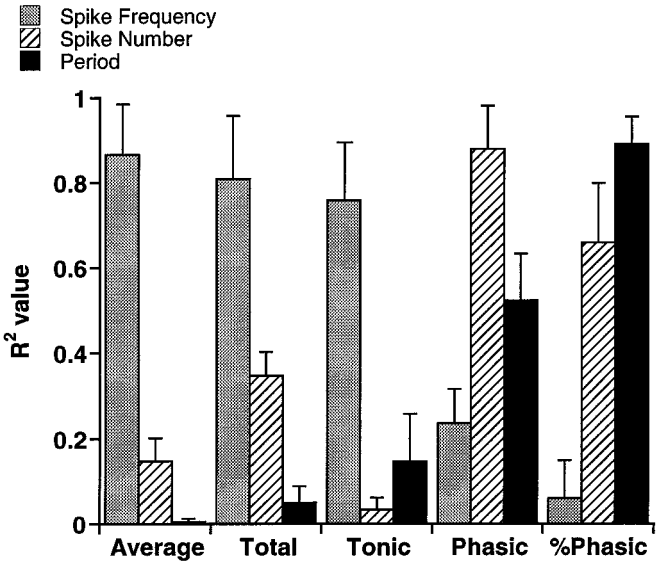

Figure 8. Mean R^2 values (5 experiments) of the various linear fits shown in Fig. 7. Average, total, and tonic amplitudes are best coded by intraburst spike frequency ($R^2 = 0.87 \pm 0.12$, 0.81 ± 0.15, and 0.76 ± 0.14, respectively), phasic amplitude by spike number ($R^2 = 0.88 \pm 0.10$), and percent phasic by cycle period ($R^2 = 0.89 \pm 0.07$). The large apparent contributions of period to phasic amplitude, and of spike number to percent phasic, are again likely due to the intercorrelation of spike number and period, because addition of period to multiple step-wise regressions of phasic amplitude resulted in only negligibly small R^2 increases, and multiple step-wise regressions of percent phasic entered only period into the model (see Results).

able to the greater interburst interval present in longer periods, which allows the muscle to relax more fully between contractions.

Although muscle contraction coding in duty cycle constant conditions is explained reasonably by the neural input parameters presented here, this by no means proves that muscle response depends only on these parameters or that all possible parameters have been investigated. In particular, in this work, duty cycle was held constant. In duty cycle constant trains, overall spike frequency (average spike frequency over the cycle period; ($sp^{\#} - 1$)/*period*) and intraburst spike frequency are proportional, as are also burst duration, interburst interval, and cycle period. Our data therefore cannot distinguish the individual elements in these two sets, and thus varying duty cycle may reveal (1) other parameters that more generally code muscle response, (2) dependencies of muscle response on as yet untested parameters, and (3) dependency on multiple parameters.

DISCUSSION

Slow, non-twitch muscles are found in lower vertebrates and invertebrates, and often participate in rapid motor patterns as well as the slow and postural behaviors with which they are often associated. We have shown here that isotonic contractions of one pair of slow muscles, the dorsal dilator muscles of the crustacean stomatogastric system, show intercontraction temporal summation in response to physiologically relevant rhythmic input. When cycle period decreases and duty cycle is kept constant, muscle contraction becomes increasingly tonic and is almost completely so at the fastest physiological period. We have identified five components of temporally summated contractions: average, total, phasic, and tonic contraction amplitudes, and the ratio of phasic to total components, percent phasic. These components are coded by different aspects of the input of the muscle: (1) average, total, and tonic contraction amplitudes are coded mainly by spike frequency, (2) phasic amplitude is coded primarily by spike number, and (3) percent phasic is coded primarily by cycle period.

Implications for pyloric motor function

The pyloric neural network is rhythmically active, and therefore it has been generally assumed that the pyloric muscles contract rhythmically as well. Our data suggest, however, that (with a constant load) at all cycle periods the dorsal dilator muscles maintain some level of sustained contraction. Which aspect (average amplitude, percent phasic, etc.) of these summated contractions is behaviorally important is unknown. Furthermore, in the intact animal, muscle loading is unlikely to be constant, and neuromodulatory substances may be released that reduce or abolish the tonic response of this muscle. However, our data on other pyloric muscles show that most of them also become increasingly tonic as cycle period decreases (Ellis et al., 1996; Koehnle et al., 1997) (P. I. Harness, L. G. Morris, S. L. Hooper, unpublished observations). It is thus possible that the dorsal dilator muscles (and several other pyloric muscles) may express tonic responses *in vivo*, and hence this response could be behaviorally relevant.

To appreciate this possibility, it is important to understand that the pyloric ossicles form an interconnected, box-like structure, and that none of the ossicles is attached to the carapace. Many pyloric muscles interconnect two ossicles (as opposed to the dorsal dilator muscles, which interconnect the carapace and an ossicle), and hence the contractions of these intrinsic muscles could theoretically move both ossicles. Tonic contraction of certain pyloric muscles could serve to stabilize ossicle position and thus determine which ossicles move as other muscles contract. For instance, each dorsal dilator muscle shares an ossicle with an intrinsic muscle (one of the bilaterally paired p1 muscles) that contracts in a later phase of the pyloric pattern. Tonic dorsal dilator muscle contraction may serve to stabilize the common ossicle throughout the pyloric cycle and hence ensure that p1 muscle contractions instead move the other ossicle to which this muscle attaches.

In light of these data, it may also be necessary to reconsider the functions of the dorsal and ventral (cpv2b) dilator muscle pairs. Each of these muscle pairs is innervated by the PD neurons, and the two pairs insert on opposite sides of the pylorus. Cocontraction of these muscle pairs was thought to dilate the pyloric chamber and open the cardiopyloric valve (Turrigiano and Heinzel, 1992). Our data, however, indicate that the contractions of these muscle pairs may be very different at fast cycle periods [under experimental conditions identical to those used here, ventral dilator muscles are phasic at all periods (Morris and Hooper, 1996)]. These observations thus suggest that (1) the ventral dilator muscles alone may open the valve (if the valve opens and closes each cycle at all periods) or (2) if the dorsal dilators do help open the valve, at fast periods the valve remains partially open (due to dorsal dilator muscle tonic contraction) throughout the cycle.

Implications for other systems

Many neuromuscular preparations show temporal summation of isometric or isotonic contractions in response to rhythmic input. Most researchers, however, have not characterized the properties of this summation or considered its possible function. Instead, researchers have generally sought mechanisms that diminish tem-

poral summation so as to preserve motor rhythmicity. These mechanisms typically involve neuromodulator-induced increases in muscle relaxation rate and have been observed in leech longitudinal muscle (Mason and Kristan, 1982) and in *Aplysia* pedal (Hall and Lloyd, 1990, McPherson and Blankenship, 1992) and accessory radula closer muscles (Weiss et al., 1992). However, in some preparations summation may be behaviorally appropriate. In particular, summation could provide finer motor control by allowing antagonistic muscle co-contraction (Bizzi and Abend, 1983) or promote stiffness in, or transmit mechanical force to, particular regions of the organism or structure (Altringham et al., 1993).

Leech (*Hirudo*) longitudinal body wall muscles are slow enough that temporal summation would likely occur in the absence of compensatory mechanisms (Mason and Kristan, 1982). This would result in antagonist co-contraction during swimming. *A priori*, such co-contraction might be considered contrary to function, and indeed the relaxation rate of these muscles can be increased (and hence temporal summation decreased) by serotonin release from the Retzius cells (Leake, 1986). However, some level of temporal summation during leech swimming may promote function, because the resulting co-contraction would increase body stiffness. Serotonin may thus be used not to abolish co-contraction but rather to regulate it as necessary to improve function as swimming speed changes or to perform other behaviors such as burrowing.

Similarly, *Aplysia* pedal muscle (used for crawling) contractions show temporal summation *in vitro* (Hall and Lloyd, 1990; McPherson and Blankenship, 1992). Pedal peptide and serotonin both increase pedal muscle relaxation rate, which decreases temporal summation and makes the contractions become more phasic. Again, however, the role of these modulators may be to regulate, not abolish, tonic muscle contraction. The *Aplysia* foot has no ossicles or other hard skeletal structures and must rely solely on hydrostatic pressure and muscle contraction for movement; tonic contraction of certain muscles thus might form a stable mechanical substrate necessary for the expression of coordinated muscle patterns such as crawling.

The *Aplysia* accessory radula closer (ARC) neuromuscular system is perhaps the best studied of all neuromodulatory systems. As ARC muscle cycle period decreases and contraction amplitude increases, its motor neurons release multiple modulators that increase relaxation rate and hence decrease the intercontraction temporal summation that otherwise would occur. It has been hypothesized that these modulators are present to allow radula closing to continue without closer and opener muscle co-contraction as feeding strength and speed increase (Weiss et al., 1992). The radula possesses relatively hard tissues, and this hypothesis is undoubtedly largely correct. However, a certain level of closer muscle contracture nonetheless may be functionally relevant for fine control of radula opening or for additional mechanical stability, and thus again this neuromodulation may exist not to abolish but to induce an optimal level of closer muscle contracture.

Implications for motor control

We have identified five components of dorsal dilator contractions and have shown that three neural input parameters (spike number, spike frequency, and cycle period) code for various of these components. However, in duty cycle constant rhythmic trains these parameters are not independent, and thus it is impossible to control individually all muscle contraction components. For instance, if one alters percent phasic by varying input cycle period, one necessarily alters phasic amplitude due to the concomitant changes in burst spike number. Similarly, if one alters tonic amplitude (by changing intraburst spike frequency), one necessarily also alters spike number and hence phasic amplitude.

How nervous systems code slow muscle contractions is clearly complex, and our data alone cannot resolve this issue. Brezina et al. (1997) have begun considering these issues theoretically, particularly for average and total amplitude, but the effects of interactions among inputs and effectors with different time scales has received relatively little experimental attention, particularly in experimentally advantageous systems in which behavior and neuronal mechanism can be described simultaneously. Our data underscore the necessity of considering these interactions when investigating how nervous systems control behavior mediated by relatively slow effectors and suggest that some of the complexity seen in many well described neural networks may exist to deal with the control problems identified here.

Finally, it is important to note that the temporal summation issues described here are not limited to neuromuscular systems but will be present in any system in which relatively rapid rhythmic inputs drive slow effectors [e.g., second messenger or protein phosphorylation systems with relatively slow kinetics (De Koninck and Schulman, 1998) or slowly activating or inactivating conductances].

REFERENCES

Altringham JD, Wardle CS, Smith CI (1993) Myotomal muscle function at different locations in the body of a swimming fish. J Exp Biol 182:191–206.

Atwood HL (1973) An attempt to account for the diversity of crustacean muscles. Am Zool 13:357–378.

Atwood HL, Hoyle G (1965) A further study of the paradox phenomenon of crustacean muscle. J Physiol (Lond) 181:225–235.

Atwood HL, Govind CK, Jahromi SS (1977) Excitatory synapses of blue crab gastric mill muscles. Cell Tissue Res 177:145–158.

Atwood HL, Govind CK, Kwan I (1978) Nonhomogeneous excitatory synapses of a crab stomach muscle. J Neurobiol 9:17–28.

Bizzi E, Abend W (1983) Posture control and trajectory formation in single- and multi-joint arm movements. In: Motor control mechanisms in health and disease. Advances in neurology, Vol 39 (Desmedt JE, ed), pp 31–45. New York: Raven.

Brezina V, Orekhova IV, Weiss KR (1997) Control of time-dependent biological processes by temporally patterned input. Proc Natl Acad Sci USA 94:10444–10449.

Bullock TH (1943) Neuromuscular facilitation in Scyphomedusae. J Cell Comp Physiol 22:251–272.

Carrier DR (1989) Ventilatory action of the hypaxial muscles of the lizard *Iguana iguana*: a function of slow muscle. J Exp Biol 143:435–457.

De Koninck P, Schulman H (1998) Sensitivity of CaM kinase II to the frequency of Ca^{+2} oscillations. Science 279:227–230.

Ellis TA, Donath AS, Morris LG, Thuma JB, Hooper SL (1996) Motor expression of a lateral pyloric constrictor muscle. Soc Neurosci Abstr 22:131.

Govind CK, Atwood HL, Maynard DM (1975) Innervation and neuromuscular physiology of intrinsic foregut muscles in the blue crab and spiny lobster. J Comp Physiol [A] 96:185–204.

Hall JD, Lloyd PE (1990) Involvement of pedal peptide in locomotion in *Aplysia*: modulation of foot muscle contractions. J Neurobiol 21:858–868.

Harris-Warrick RM, Marder E, Selverston AI, Moulins M (1992) Dynamic biological networks: the stomatogastric nervous system. Cambridge, MA: MIT.

Hedwig B (1992) On the control of stridulation in the acridid grasshopper *Omocestus viridulus* L. II. Shaping hindleg movements by spiking and non-spiking interneurons. J Comp Physiol [A] 171:129–140.

Hetherington TE, Lombard RE (1983) Electromyography of the opercularis muscle of *Rana catesbeiana*: an amphibian tonic muscle. J Morphol 175:17–26.

Hooper SL (1997) Phase maintenance in the pyloric pattern of the lobster (*Panulirus interruptus*) stomatogastric ganglion. J Comput Neurosci 4:191–206.

Hoyle G (1953) "Slow" and "fast" nerve fibres in locusts. Nature 172:165.

Hoyle G (1983) Muscles and their neural control. New York: Wiley.

Josephson RK, Stokes DR (1987) The contractile properties of a crab respiratory muscle. J Exp Biol 131:265–287.

Koehnle TJ, Morris LG, Thuma JB, Hooper SL (1997) Motor activity of the pyloric and cardiac sac network-innervated cv1 muscle. Soc Neurosci Abstr 23:477.

Leake, LD (1986) Leech Retzius cells and 5-hydroxytryptamine. Comp Biochem Physiol [C] 83:229–239.

Mason A, Kristan Jr WB (1982) Neuronal excitation, inhibition and modulation of leech longitudinal muscle. J Comp Physiol [A] 146:527–536.

Maynard DM, Dando MR (1974) The structure of the stomatogastric neuromuscular system in *Callinectes sapidus, Homarus americanus*, and *Panulirus argus* (decapoda crustacea). Philos Trans R Soc Lond Biol Sci 268:161–220.

McPherson DR, Blankenship JE (1992) Neuronal modulation of foot and body-wall contractions in *Aplysia californica*. J Neurophysiol 67:23–28.

Morris LG, Hooper SL (1994) Dorsal dilator muscles in *Panulirus* may express both pyloric and gastric mill motor patterns. Soc Neurosci Abstr 20:1413.

Morris LG, Hooper SL (1996) The pyloric dilator muscles show very different contraction amplitude, facilitation, and summation. Soc Neurosci Abstr 22:131.

Morris LG, Hooper SL (1997) Muscle response to changing neuronal input in the lobster (*Panulirus interruptus*) stomatogastric system: spike number- versus spike frequency-dependent domains. J Neurosci 17:5956–5971.

Rome LC, Funke RP, Alexander RM, Lutz G, Aldridge H, Scott F, Freadman M (1988) Why animals have different muscle fibre types. Nature 335:824–827.

Selverston AI, Russell DF, Miller JP, King DG (1976) The stomatogastric nervous system: structure and function of a small neural network. Prog Neurobiol 7:215–290.

Selverston AI, Moulins M (1987) The crustacean stomatogastric system. Berlin: Springer.

Tu MS, Dickinson MH (1994) Modulation of negative work output from a steering muscle of the blowfly *Calliphora vicina*. J Exp Biol 192:207–224.

Turrigiano GG, Heinzel HG (1992) Behavioral correlates of stomatogastric function. In: Dynamic biological networks: the stomatogastric nervous system (Harris-Warrick RM, Marder E, Selverston AI, Moulins M, eds), pp 197–220. Cambridge, MA: MIT.

Webb PW (1994) The biology of fish swimming. In: Mechanics and physiology of animal swimming (Maddock L, Bone Q, Rayner JMV, eds), pp 45–62. Cambridge, UK: Cambridge University.

Weiss KR, Brezina V, Cropper EC, Hooper SL, Miller MW, Probst WC, Vilim FS, Kupfermann I (1992) Peptidergic cotransmission in *Aplysia*: functional implications for rhythmic behaviors. Experientia 48: 456–463.